Journal Pre-proofs

Synthesis, α-glucosidase inhibition, and molecular docking studies of novel *N*-substituted hydrazide derivatives of atranorin as antidiabetic agents

Thuc-Huy Duong, Asshaima Paramita Devi, Nguyen-Minh-An Tran, Hoang-Vinh-Truong Phan, Ngoc-Vinh Huynh, Jirapast Sichaem, Hoai-Duc Tran, Mahboob Alam, Thi-Phuong Nguyen, Huu-Hung Nguyen, Warinthorn Chavasiri, Tien-Cong Nguyen

PII: S0960-894X(20)30470-4
DOI: https://doi.org/10.1016/j.bmcl.2020.127359
Reference: BMCL 127359

To appear in: *Bioorganic & Medicinal Chemistry Letters*

Received Date: 1 March 2020
Revised Date: 25 May 2020
Accepted Date: 17 June 2020

Please cite this article as: Duong, T-H., Paramita Devi, A., Tran, N-M., Phan, H-V., Huynh, N-V., Sichaem, J., Tran, H-D., Alam, M., Nguyen, T-P., Nguyen, H-H., Chavasiri, W., Nguyen, T-C., Synthesis, α-glucosidase inhibition, and molecular docking studies of novel *N*-substituted hydrazide derivatives of atranorin as antidiabetic agents, *Bioorganic & Medicinal Chemistry Letters* (2020), doi: https://doi.org/10.1016/j.bmcl.2020.127359

Synthesis, α-glucosidase inhibition, and molecular docking studies of novel *N*-substituted hydrazide derivatives of atranorin as antidiabetic agents

Thuc-Huy Duong[a,b], Asshaima Paramita Devi[c], Nguyen-Minh-An Tran[d], Hoang-Vinh-Truong Phan[e], Ngoc-Vinh Huynh[f], Jirapast Sichaem[g,*], Hoai-Duc Tran[d], Mahboob Alam[h], Thi-Phuong Nguyen[i], Huu-Hung Nguyen[k], Warinthorn Chavasiri[c], Tien-Cong Nguyen[e,*]

[a]*Department for Management of Science and Technology Development, Ton Duc Thang University, Ho Chi Minh City, Vietnam; duongthuchuy@tdtu.edu.vn*

[b]*Faculty of Applied Sciences, Ton Duc Thang University, Ho Chi Minh City, Vietnam*

[c]*Center of Excellence in Natural Products Chemistry, Department of Chemistry, Faculty of Science, Chulalongkorn University, Pathumwan, Bangkok 10330, Thailand*

[d]*Industrial University of Ho Chi Minh City, Ho Chi Minh City, Vietnam*

[e]*Department of Chemistry, Ho Chi Minh City University of Education, 280 An Duong Vuong Street, District 5, 748342 Ho Chi Minh City, Vietnam*

[f]*Department of Organic Chemistry, VNUHCM - University of Science, Ho Chi Minh City, Vietnam.*

[g]*Research Unit in Natural Products Chemistry and Bioactivities, Faculty of Science and Technology, Thammasat University Lampang Campus, Lampang 52190, Thailand*

[h]*Division of Chemistry and Biotechnology, Dongguk University, 123 Dongdae-ro, Gyeongju 780-714, Republic of Korea*

[i]*NTT Hi-Tech Institute, Nguyen Tat Thanh University, 300A Nguyen Tat Thanh, District 4, Ho Chi Minh City, Vietnam*

[k]*Faculty of Environment and Biotechnology, Van Lang University, 45 Nguyen Khac Nhu, District 1, Ho Chi Minh City, Vietnam*

* Corresponding authors;

Dr. Jirapast Sichaem. Research Unit in Natural Products Chemistry and Bioactivities, Faculty of Science and Technology, Thammasat University Lampang Campus, Lampang 52190, Thailand.
Email: jirapast@tu.ac.th

Dr. Tien-Cong Nguyen. Department of Chemistry, Ho Chi Minh City University of Education, 280 An Duong Vuong Street, District 5, 748342 Ho Chi Minh City, Vietnam.
Email: congnt@hcmup.edu.vn

Abstract

A series of novel *N*-substituted hydrazide derivatives were synthesized by reacting atranorin, a compound with a natural depside structure (**1**), with a range of hydrazines. The natural product and 12 new analogues (**2-13**) were investigated for inhibition of *α*-glucosidase. The *N*-substituted hydrazide derivatives showed more potent inhibition than the original. The experimental results were confirmed by docking analysis. This study suggests that these compounds are promising molecules for diabetes therapy. Molecular dynamics simulations were carried out with compound **2** demonstrating the best docking model using Gromac during simulation up to 20 ns to explore the stability of the complex ligand-protein. Furthermore, the activity of all synthetic compounds **2-13** against a normal cell line HEK293, used for assessing their cytotoxicity, was evaluated.

Key words: *Parmotrema tsavoense*; atranorin; *N*-substituted hydrazide derivatives; *α*-glucosidase inhibition; cytotoxicity

Type 2 diabetes mellitus (T2DM) affects a large population worldwide. It is a serious and common chronic disease resulting from a complex inheritance-environment interaction along with other risk factors such as obesity and sedentary lifestyle. There are several classes of antidiabetic drugs to treat this disease include insulin, metformin, thiazolinediones, sulfonylureas, DPPIV inhibitors, and *α*-glucosidase inhibitors. However, it is difficult to effectively treat T2DM by single treatment option in the long term. Therefore, there is a significant unmet medical need for the development of new, long term safety and highly effective antidiabetic therapies with novel and multiple mode of action. [1]

α-Glucosidase is the enzyme that catalyzes the breakage of the *α*-1,4-glycosidic bonds of polysaccharides with concomitant conversion into glucose.[2] *α*-Glucosidase inhibitors are therapeutic agents that can reduce the level of glucose in type 2 diabetes (T2DM) by preventing the hydrolysis of glucose by *α*-glucosidase, a carbohydrate metabolizing enzyme. Acarbose is an antidiabetic drug used to treat T2DM that causes various side effects including abdominal discomfort, diarrhea, bloating, pain, and flatulence. Previous studies have shown that *α*-glucosidase can be related to diseases such as cancer and viral infections.[3] Therefore, *α*-glucosidase is an attractive target for developing drugs to treat T2DM and several *α*-glucosidase inhibitors are already in the market or in clinical trial.

Atranorin, a biologically active lichen metabolite, exhibits a wide range of biological activities, being antimicrobial, antiviral, anti-inflammatory, analgesic, and cytotoxic at levels from moderate to high.[4-6] Interestingly, it is able to inhibit enzymes involved in human diseases, including tyrosinase, glucosidase, acetylcholinesterase, and xanthine oxidase.[7-12] Atranorin is present in large amounts in the *Parmotrema* lichens.[7,13] The preparation of atranorin derivatives is receiving wide attraction. Vu and co-workers (2015) modified the aldehyde group at C-3 to yield two derivatives that were more active against the hepatitis C virus (HCV) than the parent compound.[13] Mallavadhani and co-workers (2018) prepared five analogs of atranorin by etherification, reduction, and nucleophilic addition. These compounds were evaluated for cytotoxicity to multiple cancer cell lines and were more active than atranorin itself.[14] However, few atranorin derivatives have been synthesized. We report the preparation and structural elucidation of *N*-substituted hydrazide derivatives of atranorin. Evaluation of their *α*-glucosidase inhibition as well as a molecular docking analysis and studies on the inhibitory mode of these synthetic compounds were explored. In addition, the docked complexes were refined and validated using molecular dynamics simulations to map the interactions between the protein ligand.

Atranorin (**1**) was purified from the lichens *P. tsavoense* and *P. praesorediosum*.[15-18] Having **1** in hand, *N*-subtituted hydrazine reagents (**N2-N13**) were prepared (Scheme 1) following previously reported procedures.[17-22] Nucleophilic addition between **1** and **N2-N13** was conducted in ethanol/acetic acid at 50^{o}C to yield novel derivatives **2-13**, at yield from 50-90% (Scheme 2). The chemical structures of the synthetic compounds were identified from the 1D-and 2D-NMR and HRESIMS spectra. The aldehyde proton signal at δ_H 10.36 in **1** was replaced by a singlet methine at δ_H 8.57-8.95 in **2-13**. This was assignable to an imine group. Likewise, the aldehyde group at δ_C 193.8 of atranorin was replaced by the imine group at δ_C 144.9-147.4 The structural analysis was confirmed by HMBC correlations and mass spectroscopic data.

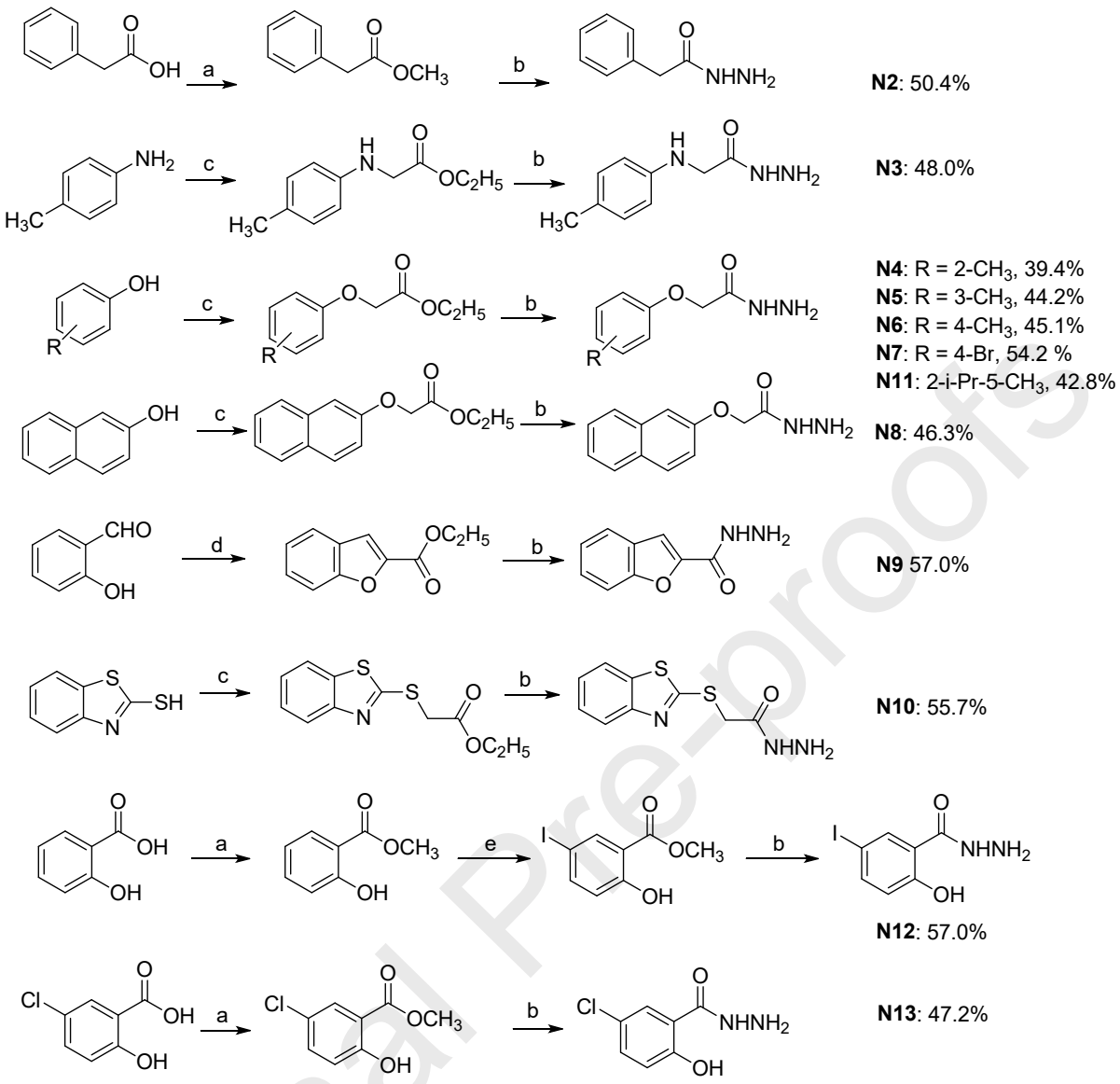

Scheme 1. Pathway to preparation of hydrazides **N2-N13**. a: CH_3OH/H_2SO_4, refluxed, 8 h; b: N_2H_4 80%/Ethanol, refluxed, 6 h; c: $ClCH_2CO_2C_2H_5/K_2CO_3$, acetone, refluxed, 24 h; d: $ClCH_2CO_2C_2H_5/K_2CO_3$, DMF, 80-90 ^oC, 3 h; e: KI/ CH_3OH, NaClO, 12 h. Overall yield.

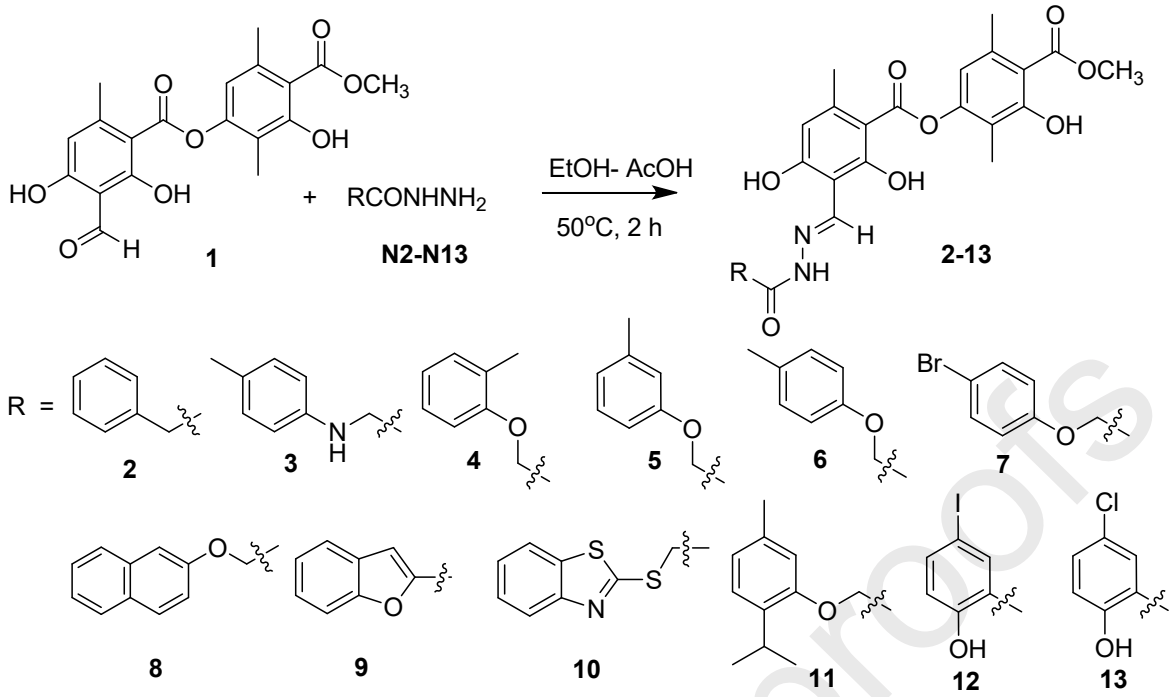

Scheme 2. Pathway to preparation of hydrazides **N2**-**N13**.

The *α*-glucosidase inhibition of **1** and all the newly synthetic compounds **2-13** was evaluated according to the literature protocol.[23] Acarbose, an *α*-glucosidase inhibitor used to treat T2DM, was chosen as a positive control for activity comparison. The results of our activity study were compiled in Table 1. As can be seen from the data in Table 1, all synthetic compounds showed potency with IC_{50} values from 6.67 to 54.71 µM. The relationship between the structure and activity was investigated. All products were more active than both the starting material (**1**) and a positive control, acarbose (IC_{50} 200 µM of **1** and 93.6 µM of acarbose). Compound **2** was the most active, indicating the important role played by the benzyl group of hydrazide **N2**. The order of potency reflected the R substituent: phenyl group (**12** and **13**) > arylamino (**3**) > aryloxy (**4**-**9**). The substituents on the R group also affected potency. The chlorine atom in **13** conferred more potency than the iodine atom in **12**. Among the aryloxy groups, the electron-donating methyl group in **4**-**6** decreased potency while the electron-withdraw bromo group in **8** increased it. Interestingly, the sulfur-containing compound **10** showed good activity, with IC_{50} value of 9.12 µM (compared to the similar scaffolds **8** and **9**). In addition, all synthetic compounds **2-13** exhibited just weak or no cytotoxicity toward HEK293 cell line (Table 2).

Table 1. *α*-Glucosidase inhibitory activity of compounds **1-13**.

No.	IC_{50}[a] (μM)	No.	IC_{50}[a] (μM)
1	>100	**8**	18.86±0.70
2	6.67±0.60	**9**	39.66±0.85
3	31.47±0.87	**10**	9.12±0.45
4	53.33±1.38	**11**	28.15±1.55
5	40.56±1.18	**12**	41.17±1.27
6	54.71±0.76	**13**	9.91±0.36
7	17.31±0.56	Acabose[b]	93.6±0.49

[a] Values are the mean ± SD. All experiments were performed at least three times.
[b] Reference compound.

Table 2. Cytotoxicity of synthetic compounds **2-13** against HEK293 cell line.

No.	IC_{50}[a] (μM)	No.	IC_{50}[a] (μM)
2	>100	**9**	84.4 ± 4.4
3	>100	**10**	70.1 ± 1.7
4	>100	**11**	>100
5	>100	**12**	94.1 ± 8.3
6	>100	**13**	63.2 ± 13.3
7	>100	Doxorucibin[b]	7.92 ± 0.07
8	52.7 ± 2.3		

[a] Values are the mean ± SD. All experiments were performed at least three times.
[b] Reference compound

In order to gain some structural insight into the inhibitory mechanisms for the *α*-glucosidase inhibitors, the binding modes in the active site were investigated. Figures 1-9 illustrates the molecular interactions of **2** and **13** with *α*-glucosidase. The IC_{50} value of **2** was 2.4 times the inhibition constant, while the free energy of binding was also negative, indicating that **2** had good inhibitory activity again enzyme **3TOP**. Ligand (**2**) docked well to **3TOP** because the free energy of binding was more negative. The IC_{50} value was also close to the estimated value. The stable conformation (**2**) formed 5 hydrogen bonds with target-receptors. These were stable hydrogen atoms in the following decreasing order :(**2**):H-A:GLN1109:OE1, 1.86 Å > A:LYS1088:HZ3-:(**2**):O, 2.00 Å > :(**2**):H-B:GLU1095:OE1, 2.01 Å > B:LYS1088:HZ2-:(2):O, 2.07 Å > A:ARG1097:HH11- :(2):O, 2.45 Å. See Table S3 and Figure 4. The hydrogen atoms in **2**, A: LYS1088, A:LYS1088, B:LYS1088, and A:ARG1097 donated, whereas those ligand (**2**) and the receptor accepted. The hydrogen bond :(**2**):H-A:GLN1109:OE1, with bond length of 1.86 Å linked

to receptor, **3TOP** compared with that of bond length of 1.61 Å B:ARG1097:HH11-:(**10**):O suggesting that hydrogen bond B:ARG1097:HH11-:(**10**):O was more stable than :(**2**):H-A:GLN1109:OE1. As shown in Figure 5, other interactions were pi-cation, pi-anion between residual amino acids, LYS A: 1088, GLU A: 1095, alkyl interactions between ILE A:1104, ARG 1097, and methyl groups of aromatic (**2**). The ligand map also exposed secondary interactions as hydrogen bonds-LYS 1088, ARG 1097, GLU 1095, and GLN 1109, steric- LYS 1088, ARG 1097, GLU 1095, GLN 1109, and THR 1101, with overlaps (Figure 6). The best conformation (**13**) linked to docking poses on **3TOP**, forming three hydrogen bonds (Table S3 and Figure 7). The most stable hydrogen bond was :(**13**):H-B:GLU1095:OE2, with a bond length of 1.86 Å: The hydrogen bond strengths ranked :(**13**):H-B:GLU1095:OE2, 1.86 Å > A:ARG1097:HH11-:(**13**):O, 2.05 Å > :(**1**):H-A:GLU1095:OE1, 2.13 Å. The donor atoms were hydrogen on A: ARG1097 and on **13**, while accepters were on receptor or conformation (**13**). The residual amino acids were highly hydrophilic: B:GLU1095, A:ARG1097, and A:GLU1095. The different interactions forming between residual amino acids of receptor-3TOP and the optimal conformation (**13**) as shown in Figure 8 as pi-cation between LYS B: 1088 and aromatic ring, alkyl, ILE B: 1104 with methyl group, pi alkyl from ILE B: 1104, ILE A: 1104 to aromatic ring, and unfavorable acceptor-acceptor from GLU A: 1095 to the nitrogen atom of azomethin (CH=N). In Figure 9, the ligand map shows hydrogen bonds between ARG1097, GLU1095, and docking poses, and steric interactions between ASP1107, ILE1104, Gly1102, GLU1095, LYS1088, and **13**.

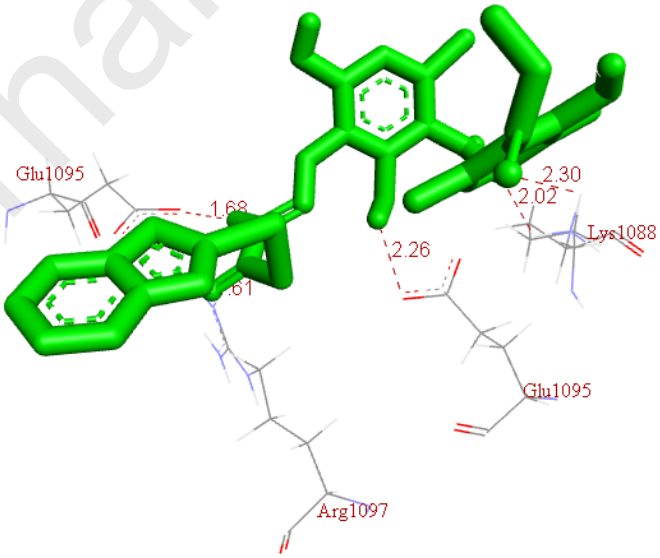

Figure 1. Binding of structure (**10**) with active sites of **3TOP**. Hydrogen bonds between residual amino acids of **3TOP** and conformation (**10**).

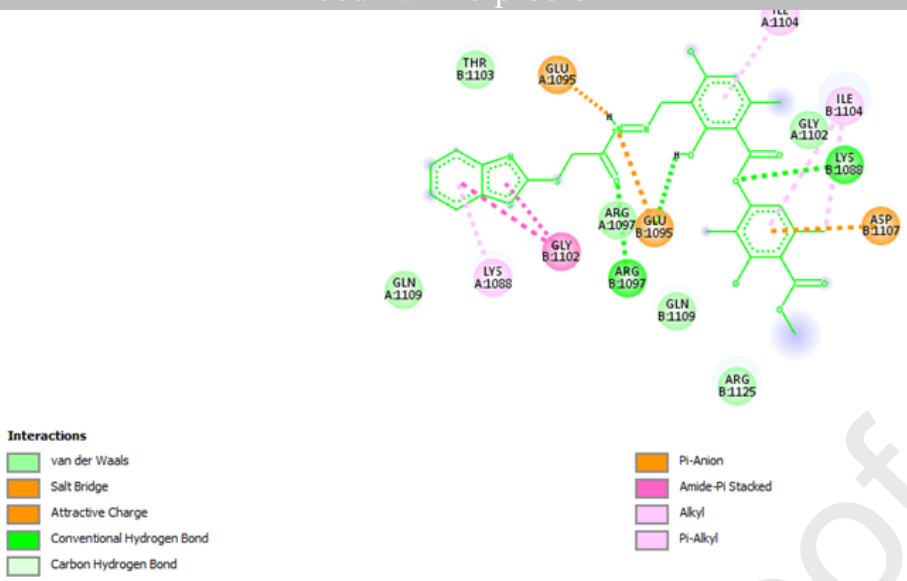

Figure 2. Interactions between receptor (**3TOP**) and stable conformation **(10)** as a 2D diagram.

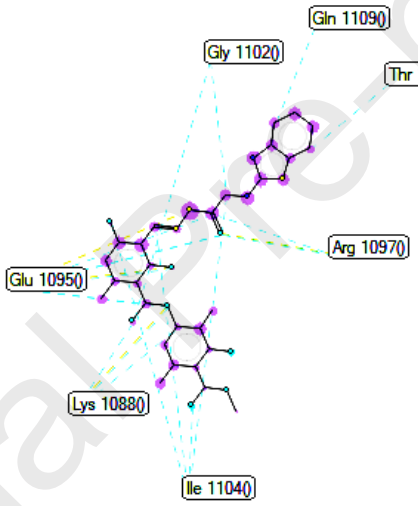

Figure 3. Ligand map showing secondary interactions to be hydrogen bonds, electrostatic, steric, and overlaps between (**10**) and docking poses of **3TOP** at 4 Å.

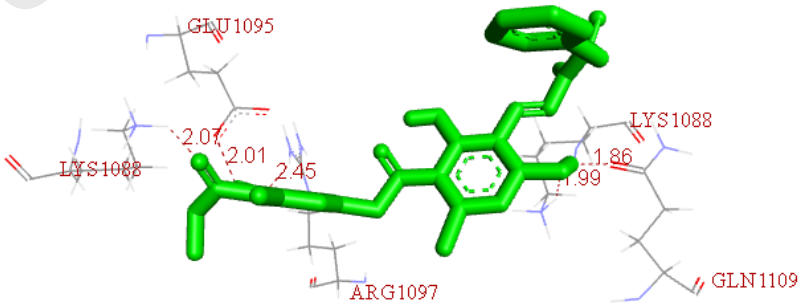

Figure 4. Binding of structure (**2**) with active sites of **3TOP**. Hydrogen bonds between residual amino acids of **3TOP** and conformation (**2**).

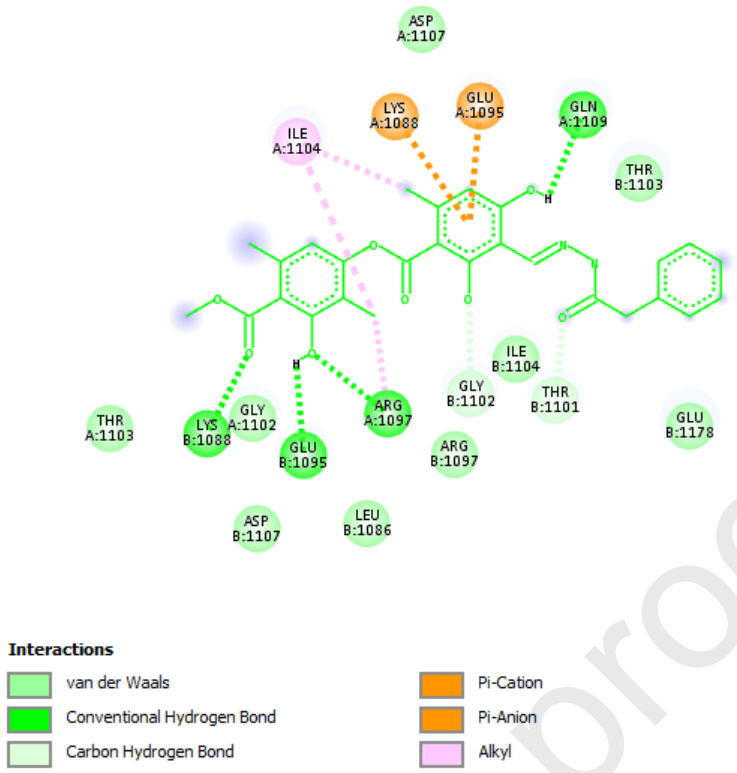

Figure 5. Interactions between receptor (**3TOP**) and the stable conformation **(2)** as a 2D diagram.

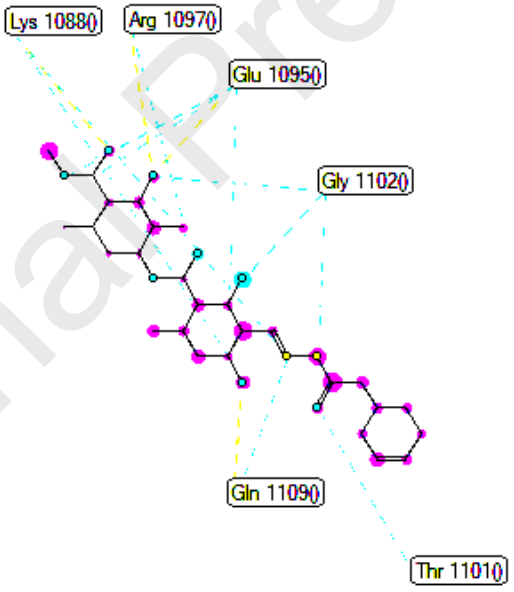

Figure 6. Ligand map showing secondary interactions to be hydrogen bonds, electrostatic, steric, and overlaps between (**2**) and docking poses of **3TOP** at 4 Å.

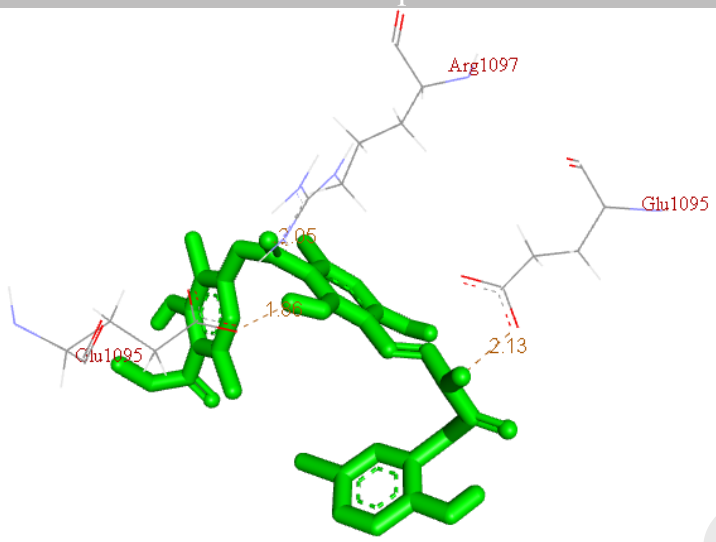

Figure 7. Binding of structure (**13**) with active sites of **3TOP**. Hydrogen bonds between residual amino acids of **3TOP** and conformation (**13**).

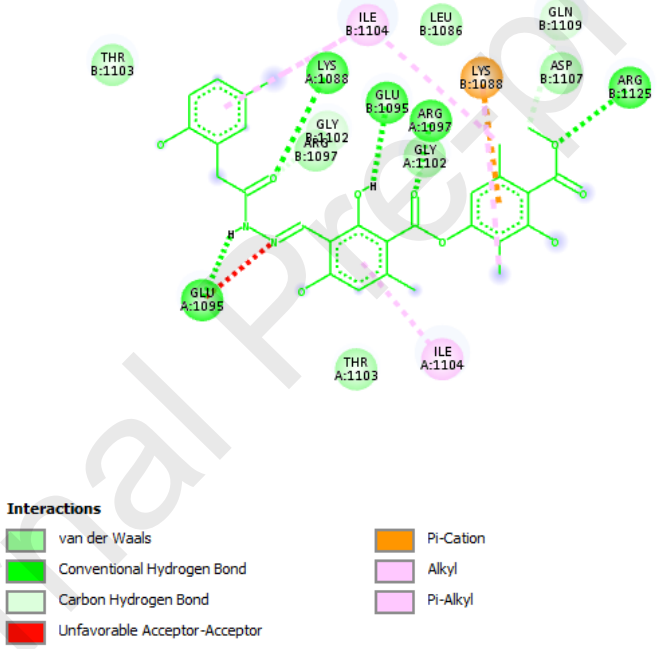

Figure 8. Interactions between receptor (**3TOP**) and stable conformation **(2)** as a 2D diagram.

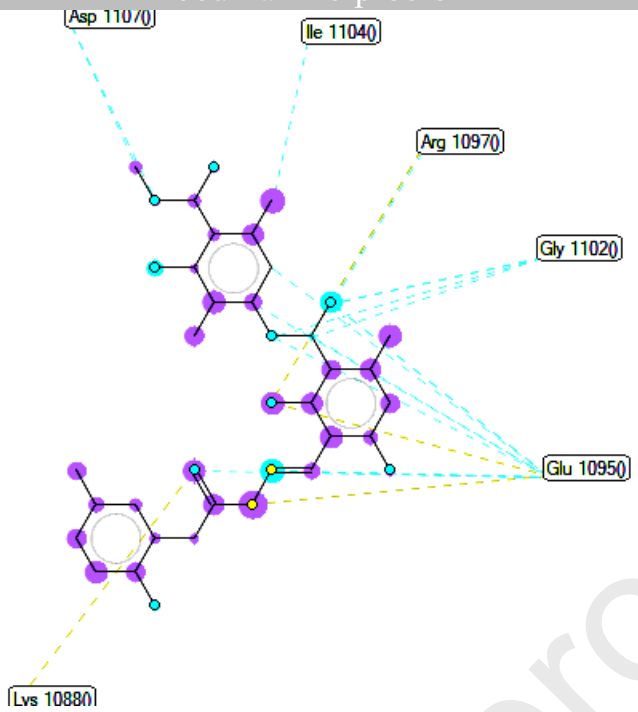

Figure 9. Ligand map showing secondary interactions to be hydrogen bonds, electrostatic, steric, and overlaps between (**13**) and docking poses of **3TOP** at 4Å.

Based on docking results, molecular dynamics (MD) simulation was performed on the selected lowest energy and best docking complex (compound **2**). Using Gromacs, we performed time-based MD simulation at 20 ns to test the durability and overall stability of the docked complexes. The residual deviations in the complexes were calculated using the RMSD graph produced by Xmgrace software. Figure 10 showed the residual deviation of the ligand docked into the receptor. The upward trend was observed in the best docked posing model with different RMSD values of 0.5-1.0 nm at 0.25 ns, followed by a downward trend of 1.0-0.75 nm at 7.5 ns, after then RMSD values in equilibrium (starting) from 7.5 to 20 ns during the simulation period. Observation from MD simulation, stable nature of compound **2** interacted complex throughout MD trajectories thereby increasing the efficiency of the docking result. The H-bond resulted in the simulation of molecular dynamics showed that, in most frames, two hydrogen bonds were found between ligand and protein structure (Figure 10B). Coulomb and Lennard-Jones (LJ) interaction potentials between the ligand (compound **2**) and the protein in the course of the simulation were considered short range types of energies obtained from MD simulation trajectory files (Figure S61a). LJ-SR is normal non-bonded interactions within the short-range cutoff (Figure S61a, red). Overall, the LJ-SR energy values ranged between −100 to −150 kJ/mol and were fairly stable. On the other hand, short-range coulomb energy values (Coul-SR) are used to know the equilibrium of the during the simulation run. Coul-SR 's energy values (Figure S61a, black) are highly fluctuated at system initialization and

indicate the system stability, but LJ-SR energies was considered rationally as binding predictors.[41] Graphs of Gromacs energy according to various parameters such as Coulomb-SR & Lennard-Jones-SR interactions, density, potential, pressure, and temperature were presented in supplementary information. The values of the parameters mentioned above were within system equilibrium limits. The parameter explications were given separately in the Figure S61 legends.

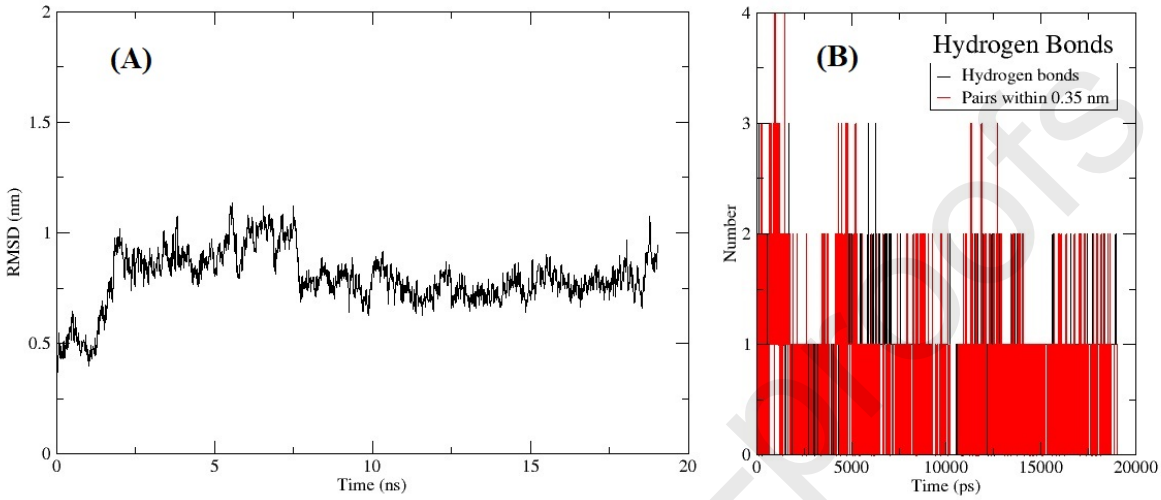

Figure 10. Analysis of the protein backbone associated with ligand (**2**) structure during simulation (A) RMSD plot; (B) Hbond distribution plot vs time.

In conclusion, we here report the synthesis of a series of novel *N*-substituted hydrazide derivatives through nucleophilic additions between **1** and *N*-subtituted hydrazine reagents. The synthesized *N*-substituted hydrazide derivative **2** showed the most powerful inhibition of yeast *α*-glucosidase (IC_{50} 6.67 μM). The potent inhibition of **2** was elaborated by molecular docking studies, in which its binding profile towards key residual amino acids in the *α*-glucosidase's active site. The simulation of the molecular dynamics was performed for compound **2** and emphasized both the affinity and stability of the ligand with the protein during contacting in the 20 ns time period. Therefore, synthetic compound **2** should hold a great potential as a leading compound for the treatment of T2DM.

Acknowledgements

This research is funded by the Foundation for Science and Technology Development of Ton Duc Thang University (FOSTECT), website: http:// fostect. tdt. edu. vn, under Grant FOSTECT.2018.04. Equipment support from Thammasat University Research Unit in Natural Products Chemistry and Bioactivities, Thammasat University, is gratefully acknowledged.

Declaration of Competing Interest

The authors declare that they have no known competing financial interests or personal relationships that could have appeared to influence the work reported in this paper.

Appendix A. Supplementary data

Supplementary data to this article can be found online at https:// doi.org/…….

References

1. Boyd RE, Valenzano KJ. Correction of lysosomal dysfunction as a therapeutic strategy for neurodegenerative diseases. Bioorganic & medicinal chemistry letters, 2014, 24(14):3001-3005.
2. Sun H, Li Y, Zhang X, Lei Y, Ding W, Zhao X, Wang H, Song X, Yao Q, Zhang Y, Ma Y. Synthesis, α-glucosidase inhibitory and molecular docking studies of prenylated and geranylated flavones, isoflavones and chalcones. Bioorgic & Medicinal Chemistry Letters, 2015, 25(20):4567-4571.
3. Adib M, Peytam F, Shourgeshty R, Mohammadi-Khanaposhtani M, Jahani M, Imanparast S, Faramarzi MA, Larijani B, Moghadamnia AA, Esfahani EN, Bandarian F. Design and synthesis of new fused carbazole-imidazole derivatives as anti-diabetic agents: *In vitro* α-glucosidase inhibition, kinetic, and in *silico* studies. Bioorganic & medicinal chemistry letters, 2019, 29(5):713-718.
4. Ranković B. Lichen secondary metabolites. Cham: Springer International Publishing. 2015.
5. Bačkorová M, Bačkor M, Mikeš J, Jendželovský R, Fedoročko P. Variable responses of different human cancer cells to the lichen compounds parietin, atranorin, usnic acid and gyrophoric acid. Toxicology in Vitro, 2011, 25(1):37-44.
6. Bačkorová M, Jendželovský R, Kello M, Bačkor M, Mikeš J, Fedoročko P. Lichen secondary metabolites are responsible for induction of apoptosis in HT-29 and A2780 human cancer cell lines. Toxicology in Vitro, 2012, 26(3):462-468.
7. Huynh BL, Le DH, Takenaka Y, Tanahashi T, Nguyen KP. New phenolic compounds from the lichen *Parmotrema praesorediosum* (Nyl.) Hale (Parmeliaceae). Magnetic Resonance in Chemistry, 2016, 54(1):81-87.
8. Behera BC, Makhija U. Inhibition of tyrosinase and xanthine oxidase by lichen species *Bulbothrix setschwanensis*. Current Science, 2002, 61-66.
9. Behera BC, Makhija U, Adawadker B. Tissue culture of *Bulbothrix setschwanensis* (lichenized ascomycetes) *in vitro.* Current Science. 2000 Apr 10;78(7):781-783.

10. Behera BC, Adawadkar B, Makhija U. Inhibitory activity of xanthine oxidase and superoxide-scavenging activity in some taxa of the lichen family Graphidaceae. Phytomedicine, 2003, 10(6-7):536-543.
11. Behera BC, Adawadkar B, Makhija U. Capacity of some Graphidaceous lichens to scavenge superoxide and inhibition of tyrosinase and xanthine oxidase activities. Current Science. 2004, 83-87.
12. Verma N, Behera BC, Sonone A, Makhija U. Lipid peroxidation and tyrosinase inhibition by lichen symbionts grown *in vitro*. African Journal of Biochemistry Research, 2008,2(12):225-231.
13. Vu TH, Le Lamer AC, Lalli C, Boustie J, Samson M, Lohézic-Le Dévéhat F, Le Seyec J. Depsides: lichen metabolites active against hepatitis C virus. PloS one, 2015, 10(3):1-14.
14. Mallavadhani UV, Somasekhar T, Sagarika G, Ramakrishna S. Isolation, chemical modification and cytotoxic evaluation of atranorin, the major metabolite of the foliose lichen *Parmotrema melanothrix.* European Chemical Bulletin, 2018, 7(4-6):150-155.
15. Duong TH, Chavasiri W, Boustie J. New meta-depsidones and diphenyl ethers from the lichen *Parmotrema tsavoense* (Krog & Swinscow) Krog & Swinscow, Parmeliaceae. Tetrahedron, 2015, 71(52):9684-9691.
16. Huynh BL, Duong TH, Do TM, Pinnock TG, Pratt LM, Yamamoto S, Watarai H, Tanahashi T, Nguyen KP. New [gamma]-Lactone Carboxylic Acids from the Lichen *Parmotrema praesorediosum* (Nyl.) Hale, Parmeliaceae. Records of Natural Products, 2016,10(3):332-340.
17. Xu FZ, Wang YY, Luo DX, Yu G, Guo SX, Fu H, Zhao YH, Wu J. Design, synthesis, insecticidal activity and 3D-QSR study for novel trifluoromethyl pyridine derivatives containing an 1,3,4-oxadiazole moiety. RSC advances, 2018, 8(12):6306-6314.
18. Rawat BS, Shukla SK, Gangwar N, Tandon R, Mehra SC. Synthesis characterization and anti-inflammatory activities of substituted aniline oxadiazolyl derivatives", International Journal of Scientific Research in Science, Engineering and Technology, 2017, 3(5):290-295.
19. Cong NT, Son TQ, Van Hien L, Thu NT. Synthesis and study of some carvone aryloxyacetylhydazones. Vietnam Journal of Chemistry, 2007, 45(2):156-161.
20. Bhardwaj B, Jain SC. Synthesis of novel *N*′-(2-oxoindolin-3-ylidene) benzofuran-2-carbohydrazides via greener approach and their biological activities. Der Pharma Chemica., 2014, 6(1):272-278.
21. Al-Omran F, El-Khair AA. Synthesis, Spectroscopy and X-Ray Characterization, of Novel Derivatives of Substituted 2-(Benzothiazol-2′-ylthio) acetohydrazide. International Journal of Organic Chemistry, 2016, 6(1):31-43.

22. Nguyen Tien C, Nguyen Van T, Le Duc G, Vu Quoc M, Vu Quoc T, Pham Chien T, Nguyen Huy H, Dang Thi Tuyet A, Van Meervelt L. Synthesis, structure and *in vitro* cytotoxicity testing of some 1, 3,4-oxadiazoline derivatives from 2-hydroxy-5-iodobenzoic acid. Acta Crystallographica Section C: Structural Chemistry, 2018, 74(7):839-846.

23. Nguyen VB, Nguyen AD, Wang SL. Utilization of fishery processing byproduct squid pens for *Paenibacillus* sp. fermentation on producing potent α-glucosidase inhibitors. Marine Drugs, 2017, 15:274.

24. Shafique S, Rashid S. structural basis of βTrCP1-associated GLI3 processing. Scientific reports, 2019, 9(1):1-3.

Declaration of Competing Interest

The authors declare that they have no known competing financial interests or personal relationships that could have appeared to influence the work reported in this paper.

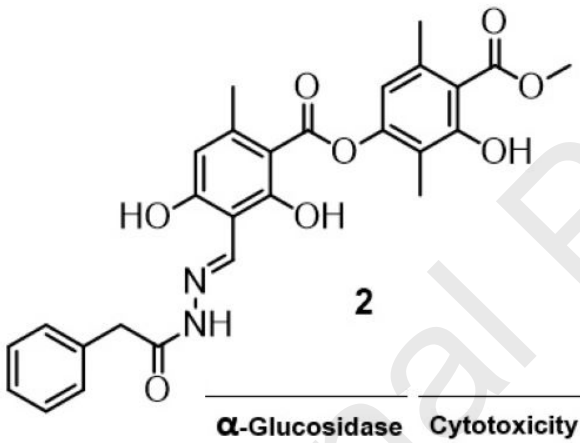

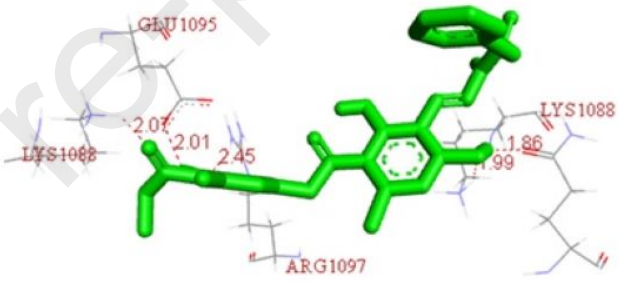

α-Glucosidase inhibition	Cytotoxicity against normal HEK293 cells
IC_{50} 6.67 μM	IC_{50} >100 μM